Finite temperature effect in infrared-improved AdS/QCD model with back reaction of bulk vacuum *

Ling-Xiao Cui(崔凌逍)[1,2,3,4;1]   Zhen Fang(房震)[1,2,3,4;2]   Yue-Liang Wu(吴岳良)[1,2,3,4;3]

[1] Key Laboratory of Theoretical Physics (SKLTP), Beijing 100190, China
[2] Kavli Institute for Theoretical Physics China (KITPC), Beijing 100190, China
[3] Institute of Theoretical Physics, Chinese Academy of Sciences, Beijing 100190, China
[4] University of Chinese Academy of Sciences (UCAS), Beijing 100049, China

Abstract: Based on an IR-improved soft-wall AdS/QCD model for mesons, which provides a consistent prediction for the mass spectra of resonance scalar, pseudoscalar, vector and axial-vector mesons, we investigate its finite temperature effect. By analyzing the spectral function of mesons and fitting it with a Breit-Wigner form, we perform an analysis for the critical temperature of mesons. The back-reaction effects of bulk vacuum are considered and the thermal mass spectral function of resonance mesons is calculated based on the back-reaction improved action. A reasonable melting temperature is found to be $T_c \approx 150 \pm 7$ MeV, which is consistent with the recent results from lattice QCD simulations.

Keywords: AdS/QCD, finite temperature, mass spectrum, spectral function, back-reaction

PACS: 12.38.Aw, 12.38.Lg, 11.15.Tk   **DOI:** 10.1088/1674-1137/40/6/063101

1 Introduction

The asymptotic freedom of quantum chromodynamics (QCD) [1] and the treatment of non-perturbative QCD have led to the QCD string approach, which eventually initiated the development of string theory. String theory has then motivated the AdS/CFT conjecture [2–5], which provides an alternative tool to access the gloomy non-perturbative region of QCD, that is, the so-called holographic QCD or AdS/QCD models based on AdS/CFT. These models are not perfect, with some deep-rooted issues from AdS/CFT as QCD is not a conformal field theory at low energy. There are different holographic QCD models due to different realizations and objectives. They have mainly been divided into two classes, namely top-down models and bottom-up models. The top-down models are directly constructed from string theory, and popular ones are the D3/D7, D4/D6 and D4/D8 models [6–8]. Bottom-up models such as the hard-wall model [9] and soft-wall model [10] are constructed according to properties of QCD itself from which the corresponding bulk gravity is determined. In

the hard-wall model, a sharp cutoff of the fifth dimension which corresponds to the inverse of the QCD scale Λ is given to realize QCD confinement. It contains chiral symmetry breaking but fails to give a correct Regge behaviour for the mass spectra of hadrons. To remedy this problem, in the soft-wall model, a dilaton term is put into the bulk action to replace the sharp IR cutoff of the hard-wall model. However, the resulting model cannot realize the chiral symmetry breaking phenomenon consistently. Several models have been constructed to incorporate these QCD behaviors [12–21]. These models have made numerical predictions for the mass spectra of light mesons, such as scalar, pseudoscalar, vector and axial-vector mesons. Especially, in a recent paper [15], we have constructed an alternative model in which the metric retains conformal invariance and satisfies Einstein's equation, while the bulk mass and bulk coupling of the quartic scalar interaction have a bulk coordinate z-dependence, so that the ultraviolet (UV) behavior of the model corresponds to AdS/CFT, while the infrared (IR) behavior is required from low energy QCD features which are compatible with the leading chiral dynamic model of spon-

taneous chiral symmetry breaking [22, 23]. As a consequence, we have arrived at a more consistent model with better predictions for the mass spectra of both ground and resonance states of scalar, pseudoscalar, vector and axial-vector mesons.

The finite temperature effects of holographic QCD have attracted a lot of attention. The finite temperature effects in hard-wall AdS/QCD were studied in Ref. [24]. In Refs. [25–28], the thermal spectrum of glueballs or mesons in the soft-wall AdS/QCD model was investigated. In Ref. [29], a soft-wall model for charmonium was built. The deconfinement temperature of soft-wall AdS/QCD models was calculated in Ref. [30] and found to be $T_c \approx 191$ MeV. In Refs. [31–33], the scalar glueball and light meson spectra were analyzed in the soft-wall AdS/QCD model and the critical temperature at which the meson states dissociation was found to be about 40−60 MeV. Such a low temperature is far from the deconfinement transition. It indicates that the meson state dissociation occurs in the confined QCD phase and is inconsistent with real QCD. To remedy this problem, we have investigated in Refs. [34, 35] the finite temperature effects for the soft wall AdS/QCD models with IR-deformed metric [13]. The critical temperature of meson dissociation was found to be around 200 MeV. Where the metric is modified at the IR region, the Hawking temperature of the black hole is not exactly defined as it does not satisfy the Einstein equation. Thus it is interesting to analyze the critical temperature of the IR-improved soft-wall AdS/QCD model for mesons [15], where the model incorporates both chiral symmetry breaking and linear confinement with better predictions on the mass spectra of meson states.

The paper is organized as follows. In Section 2, by briefly reviewing the IR-improved soft-wall AdS/QCD model for mesons [15], we extend it to an action with finite temperature. In Section 3, we analyze the thermal spectral function and carry out calculations for the meson thermal mass spectra. The corresponding melting temperature is obtained. In Section 4, the back-reaction effort of bulk vacuum is considered to yield an improved metric of background gravity, and the thermal mass spectra are investigated in detail based on the back-reaction improved action. A reasonable melting temperature is obtained. Our conclusions and remarks are presented in the final section.

2   IR-improved soft-wall AdS/QCD model with finite temperature

In this section, we will investigate the finite temperature behavior of the IR-improved soft-wall AdS/QCD model [15]. Here the AdS black hole is chosen as the background to describe temperature in boundary theory:

$$ds^2 = a(z)^2 \left(f(z)dt^2 - d\vec{x}^2 - \frac{dz^2}{f(z)} \right), \qquad (1)$$

with $a(z) = \dfrac{R}{z}$ and

$$f(z) = 1 - \frac{z^4}{z_h^4}, \qquad (2)$$

where z_h is the location of the outer horizon of the black hole. We will set the AdS radius as unity in this paper for the boundary theories. The Hawking temperature which corresponds to the temperature in boundary theory is defined as follows:

$$T_H = \frac{1}{4\pi} \left| \frac{df}{dz} \right|_{z \to z_h} = \frac{1}{\pi z_h}. \qquad (3)$$

The action with finite temperature is based on the IR-improved soft-wall AdS/QCD model for mesons [15]:

$$S = \int d^5x \sqrt{g} e^{-\Phi(z)} \operatorname{Tr} \Big[|DX|^2 - m_X^2 |X|^2 - \lambda_X |X|^4$$
$$- \frac{1}{4g_5^2} (F_L^2 + F_R^2) \Big] \qquad (4)$$

with $D^M X = \partial^M X - iA_L^M X + iX A_R^M$, $A_{L,R}^M = A_{L,R}^{M\,a} t^a$ and $\operatorname{Tr}[t^a t^b] = \delta^{ab}/2$. The gauge coupling g_5 is fixed to be $g_5^2 = 12\pi^2/N_c$ with N_c the color number [9]. The complex bulk field X will be written into the scalar and pseudoscalar mesons, and the combination of chiral gauge fields A_L and A_R will be identified with the vector and axial-vector mesons. It has been shown that it is reasonable for the dilaton field, bulk scalar mass and quartic interaction coupling to take the following IR-modified forms [15]:

$$\Phi(z) = \mu_g^2 z^2 - \frac{\lambda_g^4 \mu_g^4 z^4}{(1 + \mu_g^2 z^2)^3}, \qquad (5)$$

$$m_X^2(z) = -3 - \frac{2\mu_g^2 z^2 + 4\mu_g^4 z^4}{1 + \mu_g^2 z^2} + \tilde{m}_X^2(z), \qquad (6)$$

$$\lambda_X(z) = \frac{\mu_g^2 z^2}{1 + \mu_g^2 z^2} \lambda. \qquad (7)$$

The expectation value of bulk scalar field X has a z-dependent form for the two-flavor case:

$$\langle X \rangle = \frac{1}{2} v(z) \begin{pmatrix} 1 & 0 \\ 0 & 1 \end{pmatrix}. \qquad (8)$$

The bulk vacuum expectation value (bVEV) $v(z)$ with proper IR and UV boundary conditions takes the following simple form [15]:

$$v(z) = \frac{Az + Bz^3}{1 + Cz^2} \qquad (9)$$

with

$$A = m_q \zeta, \quad B = \frac{\sigma}{\zeta} + m_q \zeta C, \quad C = \mu_c^2/\zeta, \qquad (10)$$

and the coupling constant λ is related to the vacuum expectation value via the equation of motion

$$v_{\mathrm{q}} \equiv \sqrt{\frac{(2\mu_{\mathrm{g}})^2}{\lambda}} = \frac{B}{C} = \frac{\sigma}{\mu_{\mathrm{c}}^2} + m_{\mathrm{q}}\zeta \tag{11}$$

The five parameters involved are fixed from the low energy parameters of mesons [15] and their values are presented in Table 1.

Table 1.   The values of the five parameters in the IR-improved AdS/QCD model.

λ_{g}	$m_{\mathrm{q}}/\mathrm{MeV}$	$\sigma^{\frac{1}{3}}/\mathrm{MeV}$	$\mu_{\mathrm{g}}/\mathrm{MeV}$	$\mu_{\mathrm{c}}/\mathrm{MeV}$
1.7	3.52	290	473	375

3   Thermal spectral function

The bulk scalar field can be decomposed as $X(x,z) \equiv (v(z)/2 + S(x,z))\mathrm{e}^{2\mathrm{i}\pi(x,z)}$, where $S(x,z)$ is the scalar meson field and $\pi(x,z) = \pi^a(x,z)t^a$ the pseudo-scalar field. The chiral gauge fields can be combined into vector field V_{M}^a and axial-vector field A_{M}^a as

$$V_{\mathrm{M}}^a \equiv \frac{1}{2}(A_{\mathrm{L,M}}^a + A_{\mathrm{R,M}}^a), \quad A_{\mathrm{M}}^a \equiv \frac{1}{2}(A_{\mathrm{L,M}}^a - A_{\mathrm{R,M}}^a). \tag{12}$$

The equations of motion for the meson fields in momentum space are derived by the Fourier transformation as follows

$$\mathrm{V} \quad : \quad V_x''(z) + \left(\frac{a'(z)}{a(z)} + \frac{f'(z)}{f(z)} - \Phi'(z)\right)V_x'(z) + \frac{\omega^2 V_x(z)}{f^2(z)} = 0, \tag{13}$$

$$\mathrm{AV} \quad : \quad A_x''(z) + \left(\frac{a'(z)}{a(z)} + \frac{f'(z)}{f(z)} - \Phi'(z)\right)A_x'(z) + \frac{\omega^2 A_x(z)}{f^2(z)} + g_5^2\frac{v^2(z)}{z^2 f(z)}A_x(z) = 0, \tag{14}$$

$$\mathrm{PS} \quad : \quad \pi''(z) + \pi'(z)\left(\frac{3a'(z)}{a(z)} + \frac{f'(z)}{f(z)} + \frac{2v'(z)}{v(z)} - \Phi'(z)\right) + \frac{\omega^2\pi(z)}{f(z)^2} = 0, \tag{15}$$

$$\mathrm{S} \quad : \quad S''(z) + S'(z)\left(\frac{3a'(z)}{a(z)} + \frac{f'(z)}{f(z)} - \Phi'(z)\right) + S(z)\left(\frac{\omega^2}{f(z)^2} - \frac{a(z)^2 m_X^2(z)}{f(z)} - \frac{3\lambda_X(z)a(z)^2 v(z)^2}{2f(z)}\right) = 0. \tag{16}$$

Note that with the temperature increasing, the horizon of the black hole z_{h} moves from infinity to the boundary side. Thus the solutions of the equations of motion will drop into the black hole before they vanish, so that one cannot use the method of finding eigenmodes. Alternatively, we shall consider the spectral function, which is the imaginary part of the retarded Green's function. In the above equations, we have put the three-momentum to zero: $\overrightarrow{p} = 0$, which allows the retarded Green's function to be simplified as: $G_{tt}^R = 0$, $G_{xx}^R = G_{yy}^R = G_{zz}^R \equiv G^R(\omega)$. For the equation of the pseudo-scalar field, for simplicity we have ignored mixing between the axial-vector field and pseudo-scalar field, as it will not affect the finite temperature behavior discussed in Ref. [35].

Let us first check the boundary behavior of the solution. Near the UV boundary, one can extract asymptotic solutions for the above four equations Eq. (13–15). For convenience, we replace the radial coordinate z by the dimensionless variable u with $u = z/z_{\mathrm{h}}$. The two linear independent solutions are found to be:

$$\mathrm{V} \quad : \quad V_1 \to uY_1(uz_{\mathrm{h}}\omega), \quad V_2 \to uJ_1(uz_{\mathrm{h}}\omega), \tag{17}$$

$$\mathrm{AV} \quad : \quad A_1 \to uY_1\left(uz_{\mathrm{h}}\sqrt{\omega^2 - 4A^2\pi^2}\right),$$

$$A_2 \to uJ_1\left(uz_{\mathrm{h}}\sqrt{\omega^2 - 4A^2\pi^2}\right), \tag{18}$$

$$\mathrm{PS} \quad : \quad \pi_1 \to uJ_1\left(\frac{u\omega}{z_{\mathrm{h}}}\right), \quad \pi_2 \to uY_1\left(\frac{u\omega}{z_{\mathrm{h}}}\right), \tag{19}$$

$$\mathrm{S} \quad : \quad S_1 \to u^2 J_1\left(uz_{\mathrm{h}}\sqrt{2\mu_g^2 + \omega^2}\right),$$

$$S_2 \to u^2 Y_1\left(uz_{\mathrm{h}}\sqrt{2\mu_g^2 + \omega^2}\right). \tag{20}$$

Here J_1 and Y_1 are the first-kind Bessel function and second-kind Bessel function respectively. As discussed in Ref. [36], in Minkowski space-time, the choice of infalling boundary condition at the horizon selects the retarded Green's function:

$$K_- \to (1-u)^{-\mathrm{i}\frac{z_{\mathrm{h}}\omega}{4}}. \tag{21}$$

The solutions of the equations of motion can be expressed by the combination of the two independent asymptotic solutions $K_1 = (V_1, A_1, S_1, \pi_1)$ and $K_2 = (V_2, A_2, S_2, \pi_2)$ as

$$K(u) = A(\omega,q)K_1(\omega,q,u) + B(\omega,q)K_2(\omega,q,u)$$

$$\longrightarrow (1-u)^{-\mathrm{i}\frac{z_{\mathrm{h}}\omega}{4}}, \tag{22}$$

where the coefficients $A(\omega,q)$ and $B(\omega,q)$ are fixed by the IR in-falling boundary condition at the horizon. The retarded Green's function can be obtained from the dual bulk fields. As an example, for the scalar field, one writes the on-shell action which reduces to a surface term:

$$S = \int \frac{\mathrm{d}^4 p}{(2\pi)^4}\, \mathrm{e}^{-\Phi(z)} f(z) a(z)^{\frac{3}{2}} S(p,z)\partial_z S(p,z)\Big|_{z=0}^{z=z_{\mathrm{h}}}. \tag{23}$$

Following the prescription in Ref. [36], after substituting Eq. (22) into the surface term of the on-shell action, one can find that the spectral function which is related to the imaginary part of the two-point retarded Green's function is proportional to the imaginary part of $B(\omega,q)/A(\omega,q)$:

$$\rho(\omega,q) = -\frac{1}{\pi}\operatorname{Im}G(\omega,q)\,\theta(\omega^2-q^2) \propto \operatorname{Im}\frac{B(\omega,q)}{A(\omega,q)}. \quad (24)$$

The numerical results of spectral function for scalar, pseudo-scalar, vector and axial-vector mesons are shown in Fig. 1.
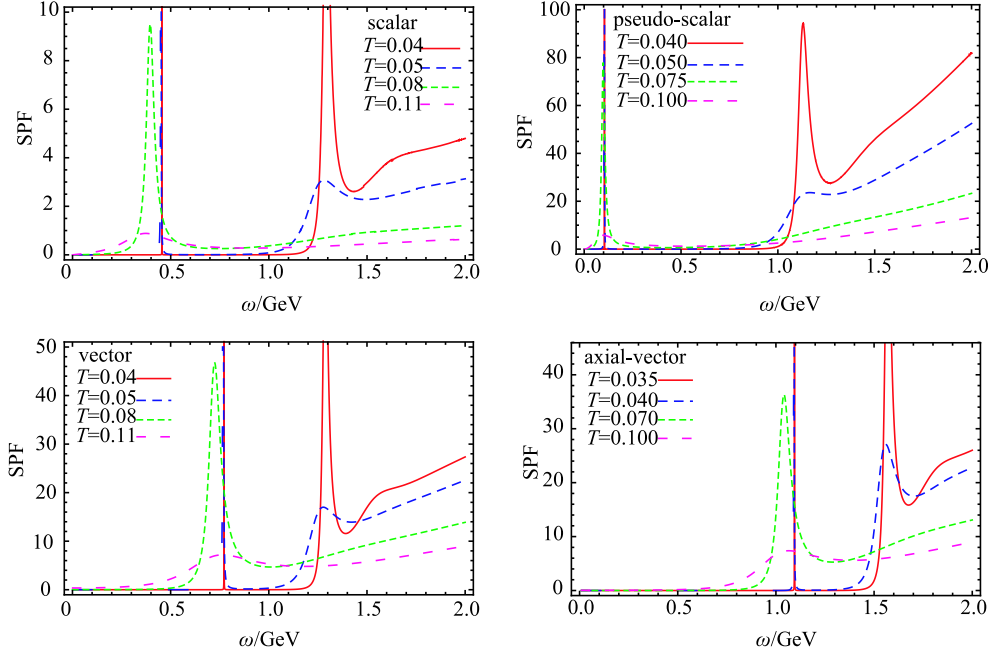
Fig. 1.   (color online) The results of the spectral function for scalar meson (top left), pseudo-scalar meson (top right), vector meson (bottom left) and axial-vector meson (bottom right).

It can be seen from the results that in the low temperature region the peaks which correspond to the poles of the Green's function represent resonance mesons with their masses coinciding to the ones given at zero temperature [15]. As the temperature increases, the meson states become unstable. This can be seen from the peaks being shifted towards smaller values and the widths becoming broader. Quantitatively, we can get more information by fitting the spectral function with a Breit-Wigner form:

$$\frac{a\omega^b}{(\omega^2-m^2)^2+\Gamma^2}+P(\omega^2), \quad (25)$$

where m and Γ are the location and width of the peak respectively. $P(\omega^2)$ represents a continuum which takes the form $P(\omega^2)=c_1+c_2\omega^2+c_3(\omega^2)^2$. The melting temperature or the critical temperature can be defined from the Breit-Wigner form. That is, if the width of a peak is larger than its height, the peak can no longer be distinguished. The condition is shown as follows:

$$h = \frac{a\omega^b}{(\omega^2-m^2)^2+\Gamma^2}\bigg|_{\omega\to m}, \qquad h<\Gamma. \quad (26)$$

Note that this definition of critical temperature is vague and subjective. In this paper, we will give the range of critical temperature by the condition: $\Gamma/2<h<\Gamma$. The range of critical temperatures of scalar, pseudo-scalar, vector and axial-vector mesons are shown in Table 2.

Table 2.   The critical temperatures of scalar, pseudo-scalar, vector and axial-vector mesons.

meson	scalar	pseudo-scalar	vector	axial-vector
T_c/MeV	133–136	135–140	136–140	143–146

The results for melting temperature imply that the mesonic quasiparticle state is dissolved around $T_c = 140$ MeV with the above considerations. The bulk coordinate z plays the role of running energy scale in boundary theory. As the Hawking temperature increases to around $T_c \approx 140$ MeV, the allowed value for z is given by $0 < z < 1/(\pi T) \approx 1/439$ MeV^{-1}. Such a small value of z will cause the bVEV $v(z)$ with $m_q \approx 0$ to approach zero as the power z^3 for the condensation σ. It can be understood that the vanishing bVEV $v(z)$ which corresponds to the chiral condensation plays an important role in the dissolving of mesonic bound states. It can be deduced that these critical behaviors could be a sign of chiral symmetry restoration.
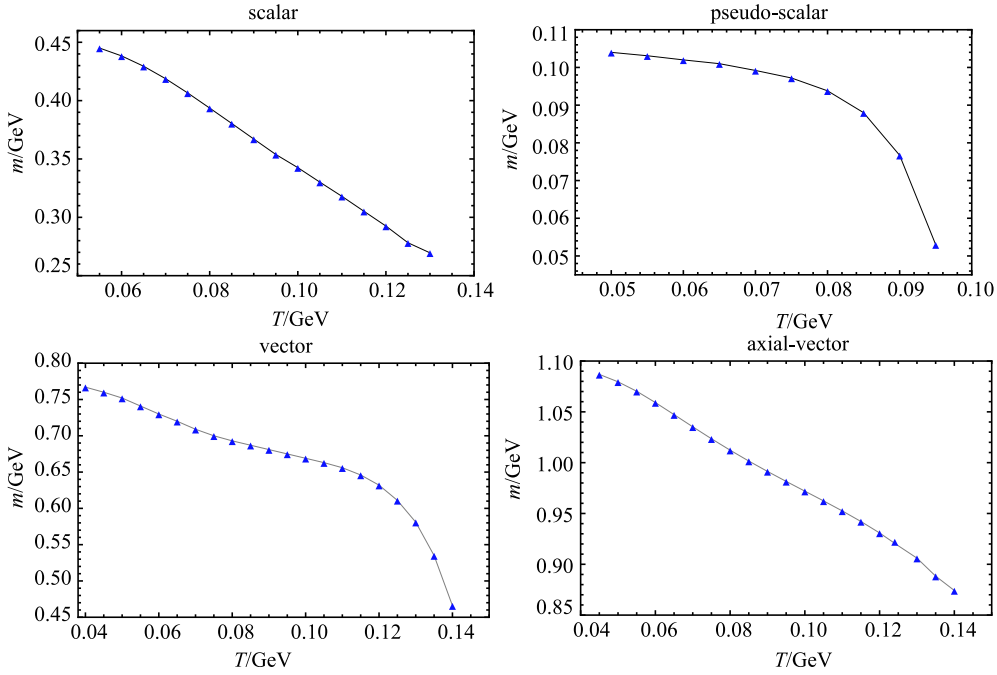
Fig. 2.   (color online) The relation between the location of the first peak and the temperature for scalar meson (top left), pseudo-scalar meson (top right), vector meson (bottom left) and axial-vector meson (bottom right).

From the Breit-Wigner form, we can quantitatively determine the relation between the mass of mesons and the temperature. The results are shown in Fig. 2.

It can be seen explicitly that as temperature increases the masses of mesons decrease linearly in the low temperature region (40–100 MeV). Note that around the critical temperature 140 MeV, the spectral function becomes so flat that the numerical fitting has a large ambiguity. It is believed that the mass of scalar and pseudo-scalar mesons will increase slightly around the critical temperature, though we cannot see that here because of the large ambiguity. For the vector and axial-vector mesons, the decrease of mass in the medium agrees with other analyses [37–39]. The more precise way to study the dependencies of temperature is to calculate the quasinormal modes of mesons. We leave this for future study.

4   Back-reaction effects of bulk vacuum

In this section, we will investigate the back-reaction effects of bulk vacuum which includes the quark mass and condensate. In Ref. [40], a fully back-reacted holographic QCD has been constructed. It was found that the back reaction has only small effects on meson spectra. It is interesting to check its influence on mass spectra with finite temperature. Let us begin with the following 5D action:

$$S = \int \mathrm{d}^5 x \sqrt{\hat{g}}\left(-\hat{R} + \mathrm{Tr}\left[|DX|^2 + V(X)\right]\right). \quad (27)$$

For simplicity we do not take the dilaton field into account in the action. $\hat{R}$ is the five dimensional Ricci scalar. X is the bulk scalar field in Eq. (4) with the bulk vacuum expectation form $X = \dfrac{1}{2}v(z)\mathbf{1}_2$. The bVEV $v(z)$ relates to quark mass and condensates in Eq. (9) and Eq. (10). After taking the trace, the action is rewritten as follows:

$$S = \int \mathrm{d}^5 x \sqrt{\hat{g}}\left(-\hat{R} + \frac{1}{2}\partial_M v \partial^M v + V(v)\right) \quad (28)$$

with $V(v) = \mathrm{Tr}\left[V(X)\right]$. To obtain the black hole solution, we consider the deformed AdSBH background:

$$\mathrm{d}s^2 = \frac{\mathrm{e}^{2A(z)}}{z^2}\left(f(z)\mathrm{d}t^2 - \mathrm{d}\vec{x}^2 - \frac{\mathrm{d}z^2}{f(z)}\right). \quad (29)$$

The equations of motion are

$$\frac{1}{2}\hat{g}_{MN}\left(-\hat{R} + \frac{1}{2}\partial_P v \partial^P v + V(v)\right)$$
$$+ \hat{R}_{MN} - \frac{1}{2}\partial_M v \partial_N v = 0, \quad (30)$$

$$\frac{\partial V(v)}{\partial v} - \frac{1}{\sqrt{\hat{g}}}\partial_M\left(\sqrt{\hat{g}}\hat{g}^{MN}\partial_N v\right) = 0. \quad (31)$$

The (t,t), (x_1,x_1) and (z,z) components of the gravitational field equations are respectively

$$A'' + A'\left(\frac{f'}{2f} - \frac{2}{z}\right) + A'^2 + \frac{2}{z^2} + \frac{v'^2}{12} - \frac{f'}{2zf} - \frac{\mathrm{e}^{2A}V(v)}{6z^2 f} = 0, \quad (32)$$

$$f'' + f'\left(6A' - \frac{6}{z}\right) + f\left(6A'' + 6A'^2 + \frac{1}{2}v'^2 + \frac{12}{z^2} - \frac{12A'}{z}\right)$$

$$- \frac{e^{2A}V(v)}{z^2} = 0, \tag{33}$$

$$A'^2 + A'\left(\frac{f'}{4f} - \frac{2}{z}\right) + \left(\frac{1}{z^2} - \frac{e^{2A}V(v) + 3zf'}{12z^2f} - \frac{v'^2}{24}\right) = 0. \tag{34}$$

From Eq. (33) and Eq. (34) we can obtain the equation of the warped factor:

$$A'' - A'^2 + \frac{2}{z}A' + \frac{1}{6}v'^2 = 0. \tag{35}$$

This equation cannot be analytically solved with the bVEV $v(z)$ given in Eq. (9). We then numerically solve $A(z)$ by using the UV boundary condition $A(0) = 0$ and its derivative vanishes for a general situation.

From Eq. (32) and Eq. (33), one can analytically solve $f(z)$ as

$$f(z) = C_1 + C_2 \int_0^z e^{-3A(z)} z^3 dz, \tag{36}$$

where C_1 and C_2 are integral constants. Near the boundary $z \to 0$, we require the metric to be asymptotic to AdS$_5$:

$$f(0) = 1. \tag{37}$$

Near the horizon $z = z_h$, we require

$$f(z_h) = 0. \tag{38}$$

Solution of $f(z)$ can be expressed as

$$f(z) = 1 - \frac{\displaystyle\int_0^z x^3 e^{-3A(x)} dx}{\displaystyle\int_0^{z_h} x^3 e^{-3A(x)} dx}. \tag{39}$$

One can expand $f(z)$ at the UV boundary with requiring $A(0) = 0$,

$$f(z \to 0) = 1 - \frac{z^4}{4 \displaystyle\int_0^{z_h} e^{-3A(t)} t^3 dt} + \cdots. \tag{40}$$
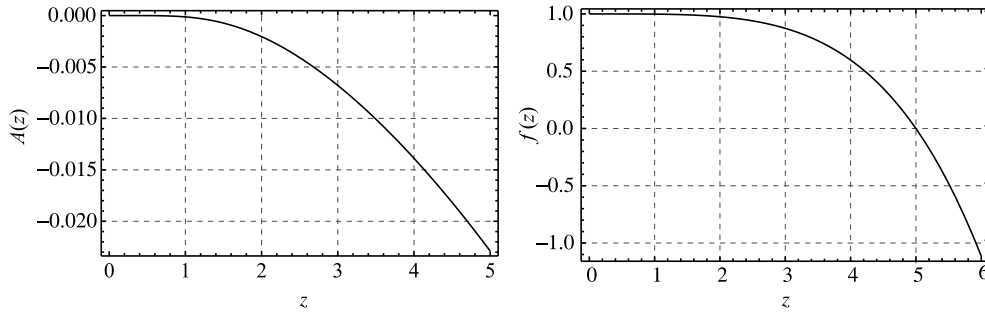
Fig. 3.   (color online) The numerical solution for $A(z)$ (left side) and $f(z)$ with horizon $z_h = 5$ (right side).

Comparing with the AdS black-hole solution, it can be seen that the correction of back-reaction contributes to the higher order terms of $f(z)$. The numerical results of $A(z)$ and $f(z)$ are presented in Fig. 3.

It is easy to obtain the Hawking temperature:

$$T_H = -\frac{1}{4\pi} \frac{\partial f}{\partial z}\Big|_{z \to z_h} = \frac{z_h^3 e^{-3A(z_h)}}{4\pi \displaystyle\int_0^{z_h} e^{-3A(x)} x^3 dx}. \tag{41}$$

We plot the temperature T_H v.s. horizon z_h in Fig. 4. The monotonic behavior indicates that such a black hole solution is stable.

With the above analysis, we are now in a position to investigate the finite temperature behavior of mesons after considering the back-reaction effects of bulk vacuum. The action has the same form as Eq. (4) except for the background metric, which has been replaced by the back-reaction improved metric $\hat{g}$:

$$S = \int d^5x \sqrt{\hat{g}} e^{-\Phi(z)} \text{Tr}\Big[|DX|^2 - m_X^2 |X|^2 - \lambda_X |X|^4$$

$$- \frac{1}{4g_5^2}(F_L^2 + F_R^2)\Big]. \tag{42}$$
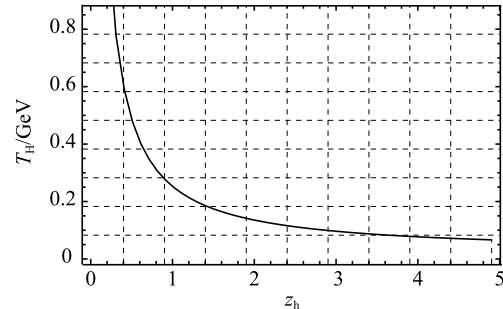
Fig. 4.   (color online) The relation between temperature T_H and horizon z_h.

Doing a similar calculation as that in Section 3, we obtain the mesons' thermal spectral function with back-reaction improved gravity background. The numerical results are shown in Fig. 5. In the low temperature region the locations of the peaks are nearly the same as those without back-reaction effects in Section 3. Such phenomena agree well with the conclusion in Ref. [40]. It is found that the warped factor $A(z)$ shown in Fig. 3 can be fitted well by a simple form $A(z) = -k^2 z^2$ with k around $k \approx 30$ MeV.
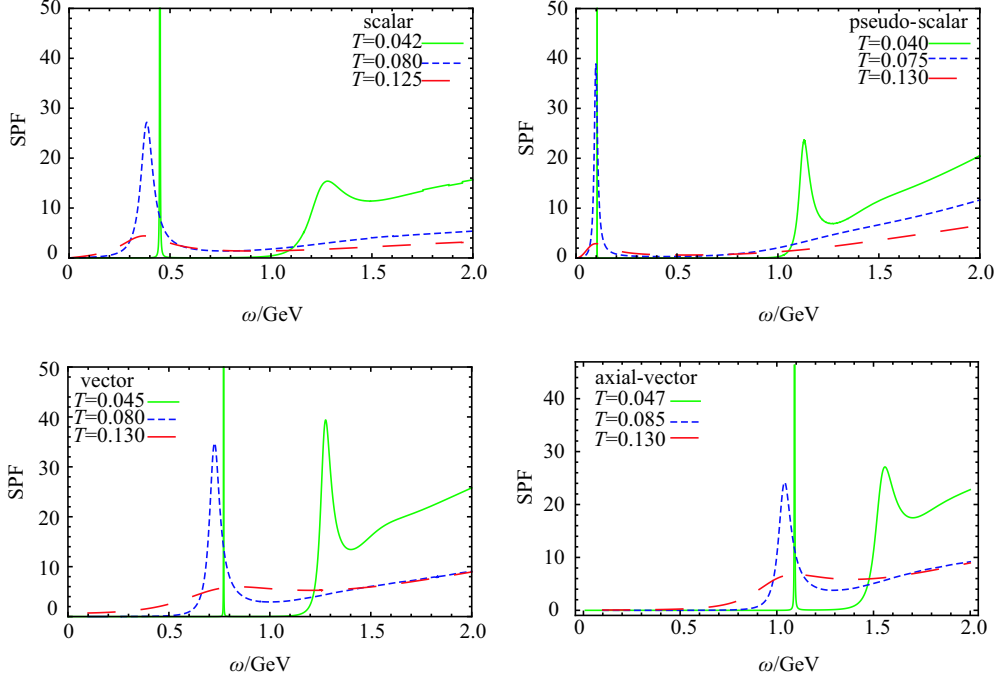
Fig. 5.   (color online) The results of spectral function for scalar meson (top left), pseudo-scalar meson (top right), vector meson (bottom left) and axial-vector meson (bottom right) with back-reaction effects.

In the zero temperature region $f(z) \approx 1$ and the back-reaction correction of quark mass and condensate has very little effect on the mass spectra. In the high temperature region, however, the melting temperatures have increased by about 10 MeV. By fitting the spectral function with the Breit-Wigner form in Eq. (25), we can obtain the critical temperature including the back-reaction effects of bulk vacuum. The results are presented in Table 3.

Table 3.   The critical temperatures of scalar, pseudo-scalar, vector and axial-vector mesons with back-reaction effects.

meson	scalar	pseudo-scalar	vector	axial-vector
T_{c}/MeV	142–147	143–148	148–152	151–157

In the above calculation the dilaton field in the action Eq.(28) is still taken as a pure background field. The back reaction effects of bulk vacuum which includes quark mass and quark condensate have increased the melting temperature to around

$$T_{c} \approx 150 \pm 7 \text{ MeV}. \qquad (43)$$

Such a result is consistent with results yielded from lattice QCD simulations. In Ref. [41], the chiral and deconfinement critical temperatures were found to be 147–157 MeV. In Ref. [42], the chiral transition temperature of two massless flavors was shown to be $T_{c} = 154 \pm 9$ MeV. For physics masses of three flavor quarks, the chiral transition temperature was found to be $T_{c} = 155$ MeV [43].

5   Conclusions and remarks

We have investigated the finite temperature behavior of the IR-improved soft-wall AdS/QCD model for mesons [15]. The spectral function of mesons has been analyzed following the prescription in Ref. [36]. By fitting the spectral function with a Breit-Wigner form, the critical temperature of mesons was found to be around 140 MeV. It has been noticed that in the low temperature region, the peaks which correspond to the poles of the Green's function are consistent with the masses calculated in the zero temperature case [15]. We would like to point out that the definition of critical temperature is vague. In obtaining the critical temperature, we have to take a range of melting temperatures with the

condition between the height (h) and width (Γ) of peak that $\Gamma/2 < h < \Gamma$. We have considered the back-reaction effects of bulk vacuum and yielded an improved metric of background gravity. The mesons' thermal mass spectral function has been calculated based on the back-reaction improved action, which leads to the critical temperature increasing by about 10 MeV. A reasonable melting temperature has been found to be $T_{\rm c} \approx 150\pm7$ MeV, which is consistent with recent results obtained from lattice QCD simulations.

References

1   D. J. Gross and F. Wilczek, Phys. Rev. Lett., **30**: 1343 (1973); H. D. Politzer, Phys. Rev. Lett. **30**, 1346 (1973)
2   J. M. Maldacena, Adv. Theor. Math. Phys., **2**: 231 (1998) [hep-th/9711200]
3   S. S. Gubser, I. R. Klebanov, and A. M. Polyakov, Phys. Lett. B **428**, 105 (1998) [hep-th/9802109]
4   E. Witten, Adv. Theor. Math. Phys., **2**: 253 (1998) [hep-th/9802150]
5   J. Polchinski and M. J. Strassler, Phys. Rev. Lett., **88**: 031601 (2002) [hep-th/0109174]
6   M. Kruczenski, D. Mateos, R. C. Myers, and D. J. Winters, JHEP, **0405**: 041 (2004) [hep-th/0311270]
7   T. Sakai and S. Sugimoto, Prog. Theor. Phys., **113**: 843 (2005) [hep-th/0412141]
8   T. Sakai and S. Sugimoto, Prog. Theor. Phys., **114**: 1083 (2005) [hep-th/0507073]
9   J. Erlich, E. Katz, D. T. Son, and M. A. Stephanov, Phys. Rev. Lett., **95**: 261602 (2005) [hep-ph/0501128]
10 A. Karch, E. Katz, D. T. Son and M. A. Stephanov, Phys. Rev. D, **74**: 015005 (2006) [hep-ph/0602229]
11 P. Colangelo, F. De Fazio, F. Giannuzzi, F. Jugeau, and S. Nicotri, Phys. Rev. D, **78**: 055009 (2008) [arXiv:0807.1054 [hep-ph]]
12 T. Gherghetta, J. I. Kapusta, and T. M. Kelley, Phys. Rev. D, **79**: 076003 (2009) [arXiv:0902.1998 [hep-ph]]
13 Y. Q. Sui, Y. L. Wu, Z. F. Xie, and Y. B. Yang, Phys. Rev. D, **81**: 014024 (2010) [arXiv:0909.3887 [hep-ph]]
14 Y. Q. Sui, Y. L. Wu, and Y. B. Yang, Phys. Rev. D, **83**: 065030 (2011) [arXiv:1012.3518 [hep-ph]]
15 L. -X. Cui, Z. Fang, and Y. -L. Wu, arXiv:1310.6487 [hep-ph]
16 A. Vega and I. Schmidt, Phys. Rev. D, **82**: 115023 (2010) [arXiv:1005.3000 [hep-ph]]
17 A. Vega and I. Schmidt, Phys.Rev. D, **84**: 017701 (2011) [e-Print: arXiv:1104.4365]
18 D. Li, M. Huang, and Q. S. Yan, Eur. Phys. J. C, **73**: 2615 (2013) [arXiv:1206.2824 [hep-th]]
19 S. J. Brodsky and G. F. de Teramond, Phys. Rev. Lett., **96**: (2006) 201601 [arXiv:hep-ph/0602252]
20 S. J. Brodsky and G. F. de Teramond, Phys. Rev. D, **77**: 056007 (2008) [arXiv:0707.3859 [hep-ph]]
21 S. J. Brodsky and G. F. de Teramond, arXiv:0909.3899 [hep-ph]; G. F. de Teramond and S. J. Brodsky, arXiv:0909.3900 [hep-ph]
22 Y. Nambu, Phys. Rev. Lett., **4**: 380 (1960)
23 Y. B. Dai and Y. L. Wu, Eur. Phys. J. C, **39**: (2005) S1 [arXiv:hep-ph/0304075]
24 K. Ghoroku, M. Yahiro, Phys. Rev. D, **73**: 125010 (2006) [hep-ph/0512289]
25 M. Fujita, K. Fukushima, T. Misumi, and M. Murata, Phys. Rev. D, **80**: 035001 (2009) [arXiv:0903.2316 [hep-ph]]
26 M. Fujita, T. Kikuchi, K. Fukushima, T. Misumi, and M. Murata, Phys. Rev. D, **81**: 065024 (2010) [arXiv:0911.2298 [hep-ph]]
27 A. S. Miranda, C. A. Ballon Bayona, H. Boschi-Filho, and N. R. F. Braga, JHEP, **0911**: 119 (2009) [arXiv:0909.1790 [hep-th]]
28 P. Colangelo, F. Giannuzzi, and S. Nicotri, Phys. Rev. D, **80**: 094019 (2009) [arXiv:0909.1534 [hep-ph]]
29 H. R. Grigoryan, P. M. Hohler, and M. A. Stephanov, Phys. Rev. D, **82**: 026005 (2010) [arXiv:1003.1138 [hep-ph]]
30 C. P. Herzog, Phys. Rev. Lett., **98**: 091601 (2007) [hep-th/0608151]
31 A. S. Miranda, C. A. Ballon Bayona, H. Boschi-Filho, and N. R. F. Braga, JHEP, **0911**: 119 (2009) [arXiv:0909.1790 [hep-th]]
32 P. Colangelo, F. De Fazio, F. Jugeau, and S. Nicotri, Phys. Lett. B, **652**: 73-78 (2007) [hep-ph/0703316].
33 P. Colangelo, F. Giannuzzi, and S. Nicotri, Phys. Rev. D, **80**: 094019 (2009). [arXiv:0909.1534 [hep-ph]]
34 L. -X. Cui, S. Takeuchi, and Y. -L. Wu, JHEP, **1204**: 144 (2012) [arXiv:1112.5923 [hep-ph]]
35 L. X. Cui and Y. L. Wu, Mod. Phys. Lett. A, **28**: No. **34**, 1350132 (2013) [arXiv:1302.4828 [hep-ph]]
36 D. T. Son and A. O. Starinets, JHEP, **0209**: 042 (2002) [hep-th/0205051]
37 E. Santini, M. D. Cozma, A. Faessler, C. Fuchs, M. I. Krivoruchenko, and B. Martemyanov, Phys. Rev. C, **78**: 034910 (2008) [arXiv:0804.3702 [nucl-th]]
38 M. Post, S. Leupold, and U. Mosel, Nucl. Phys. A, **741**: 81 (2004) [nucl-th/0309085]
39 A. K. Dutt-Mazumder, R. Hofmann, and M. Pospelov, Phys. Rev. C, **63**: 015204 (2001) [hep-ph/0005100]
40 J. P. Shock, F. Wu, Y. -L. Wu, and Z. -F. Xie, JHEP, **0703**: 064 (2007) [hep-ph/0611227]
41 S. Borsanyi et al (Wuppertal-Budapest Collaboration), JHEP, **1009**: 073 (2010) [arXiv:1005.3508 [hep-lat]]
42 A. Bazavov, T. Bhattacharya, M. Cheng, C. DeTar, H. T. Ding, S. Gottlieb, R. Gupta and P. Hegde et al, Phys. Rev. D, **85**: 054503 (2012) [arXiv:1111.1710 [hep-lat]]
43 T. Bhattacharya et al, Phys. Rev. Lett., **113**: 082001 (2014) [arXiv:1402.5175 [hep-lat]]